



Australian Government
Geoscience Australia



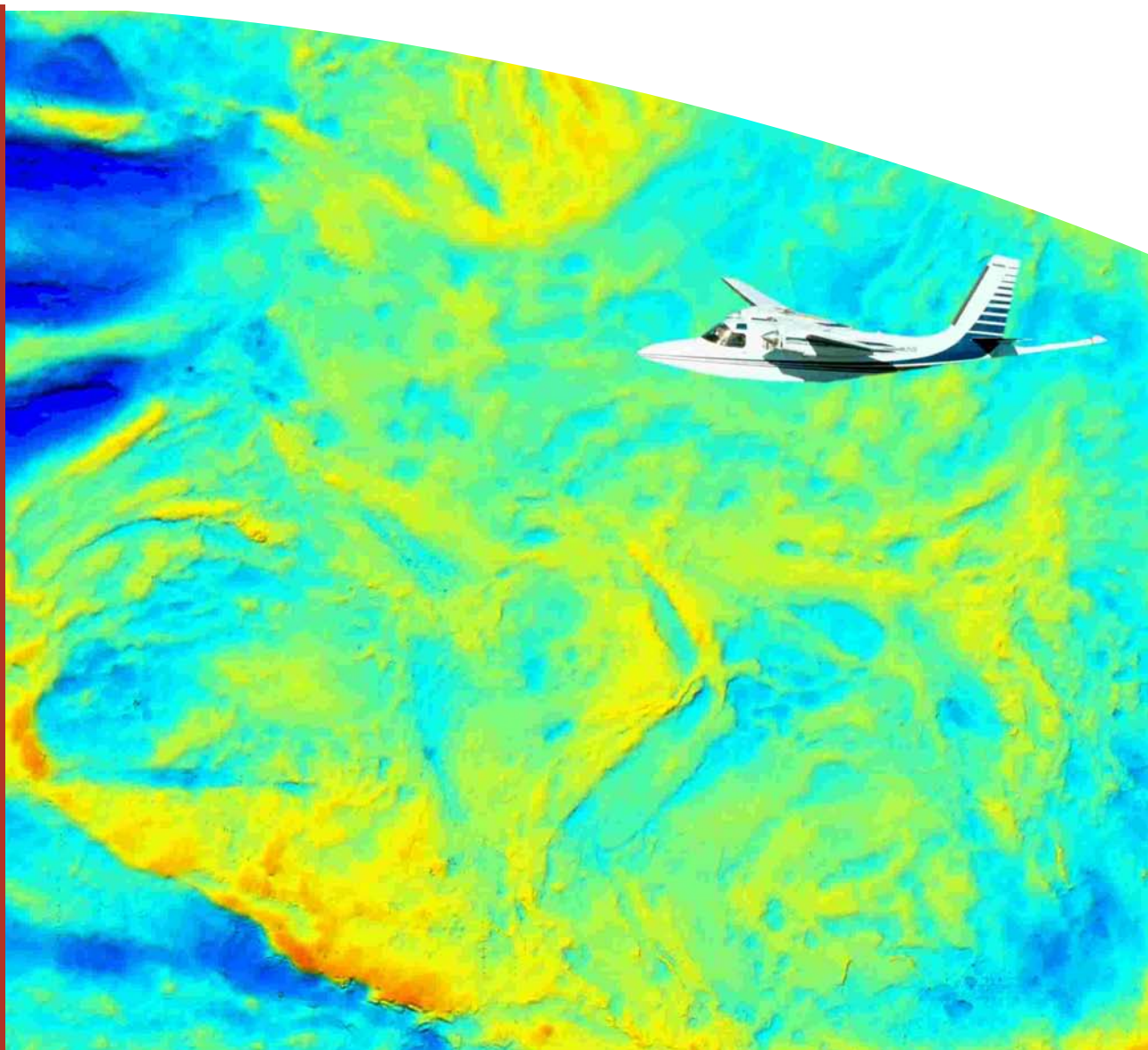
Airborne Gravity 2004

Abstracts from the ASEG-PESA
Airborne Gravity 2004 Workshop

Edited by Richard Lane

Record

2004/18



Airborne Gravity 2004

Abstracts from the ASEG-PESA
Airborne Gravity 2004 Workshop

Edited by Richard Lane

Department of Industry, Tourism & Resources

Minister for Industry, Tourism & Resources: The Hon. Ian Macfarlane, MP
Parliamentary Secretary: The Hon. Warren Entsch, MP
Secretary: Mark Paterson

Geoscience Australia

Chief Executive Officer: Neil Williams

© Commonwealth of Australia 2004

This work is copyright. Apart from any fair dealings for the purposes of study, research, criticism or review, as permitted under the Copyright Act, no part may be reproduced by any process without written permission. Inquiries should be directed to the Communications Unit, Geoscience Australia, GPO Box 378, Canberra City, ACT, 2601

ISSN: 1448-2177

ISBN: 1 920871 13 6

GeoCat no. 61129

Bibliographic Reference:

a) For the entire publication

Lane, R.J.L., editor, 2004, Airborne Gravity 2004 – Abstracts from the ASEG-PESA Airborne Gravity 2004 Workshop: *Geoscience Australia Record* 2004/18.

b) For an individual paper

van Kann, F., 2004, Requirements and general principles of airborne gravity gradiometers for mineral exploration, in R.J.L. Lane, editor, Airborne Gravity 2004 - Abstracts from the ASEG-PESA Airborne Gravity 2004 Workshop: *Geoscience Australia Record* 2004/18, 1-5.

Geoscience Australia has tried to make the information in this product as accurate as possible. However, it does not guarantee that the information is totally accurate or complete. THEREFORE, YOU SHOULD NOT RELY SOLELY ON THIS INFORMATION WHEN MAKING A COMMERCIAL DECISION.

Contents

“Airborne Gravity 2004 Workshop” Record

R.J.L. Lane, M.H. Dransfield, D. Robson, R.J. Smith and G. Walker.....v

Requirements and general principles of airborne gravity gradiometers for mineral exploration

F. van Kann.....1

The Air-FTG™ airborne gravity gradiometer system

C.A. Murphy.....7

The FALCON® airborne gravity gradiometer systems

M.H. Dransfield and J.B. Lee.....15

A superconducting gravity gradiometer tool for exploration

J.M. Lumley, J.P. White, G. Barnes, D. Huang and H.J. Paik.....21

A high resolution airborne gravimeter and airborne gravity gradiometer

B. Tryggvason, B. Main and B. French.....41

The AIRGrav airborne gravity system

S. Sander, M. Argyle, S. Elieff, S. Ferguson, V. Lavoie and L. Sander.....49

The GT-1A mobile gravimeter

A. Gabell, H. Tuckett and D. Olson.....55

A synopsis of airborne gravity data presentation, modelling, interpretation and inversion software

G. Walker.....63

Acquisition and preliminary impressions of airborne gravity gradient and aeromagnetic data in the Eastern Papuan Basin, Papua New Guinea

A. Nelson.....65

Evaluation of a full tensor gravity gradiometer for kimberlite exploration

D. Hatch.....73

Integrating ground and airborne data into regional gravity compilations

R.J.L. Lane.....81

Airborne gravity data acquisition and processing: A case study in the Prince Charles Mountains, East Antarctica

M. McLean, D. Damaske, V. Damm and G. Reitmayr.....99

AIRGrav airborne gravity survey in Timmins, Ontario

S. Elieff and S. Sander.....111

Examples of FALCON™ data from diamond exploration projects in Northern Australian

D. Isles and I. Moody.....121

A comparison of the Falcon® and Air-FTG™ airborne gravity gradiometer systems at the Kokong Test Block, Botswana

D. Hinks, S. McIntosh and R.J.L. Lane.....125

Analysis of errors in gravity derived from the Falcon® Airborne Gravity Gradiometer

D.B. Boggs and M.H. Dransfield.....135

“Airborne Gravity 2004 Workshop” Record

Richard Lane
Geoscience Australia
richard.lane@ga.gov.au

Mark Dransfield
BHP Billiton
Mark.H.Dransfield@bhpbilliton.com

David Robson
NSW Department of Primary Industry – Minerals
david.robson@minerals.nsw.gov.au

Robert Smith
Greenfields Geophysics
greengeo@bigpond.net.au

Greg Walker
BHP Billiton
Greg.B.Walker@BHPBilliton.com

Preface

The "Airborne Gravity 2004 Workshop" was held in Sydney on August 15, in conjunction with ASEG-PESA Sydney 2004 (the ASEG's 17th Geophysical Conference and Exhibition). The aims of the workshop were to provide participants with a review of the current state of the art in airborne gravity instrumentation, to present case histories of the use of these methods in minerals and petroleum applications, and to distribute sample data sets. "Airborne gravity" is used in this context to include both airborne gravimeter and airborne gravity gradiometer methods.

The program was split into 2 sessions. The morning session provided a review of the systems, with presentations covering a number of systems currently in operation as well as some that are still under development. The focus shifted in the afternoon session to case histories, with examples from surveys spanning the globe; from Antarctica to the tropics of Papua New Guinea, from Africa through Australia to Canada.

To capture the essence of the day and to promote the ongoing development of airborne geophysical methods, speakers were invited to submit papers for inclusion in a workshop volume. The papers were reviewed prior to publication in this Geoscience Australia Record. Participants received a copy at the workshop, and additional copies of the Record are available on an ongoing basis from Geoscience Australia (www.ga.gov.au).

Units

Physical quantities should be expressed in SI units. The Bureau International des Poids et Mesures (BIPM) is the custodian of this system. To quote from their website (www.bipm.fr): "Its mandate is to provide the basis for a single, coherent system of measurements throughout the world, traceable to the International System of Units (SI)".

The SI unit for acceleration is "metre per second squared" (m/s^2). The signals encountered in gravity surveys for exploration are small, and the prefix "micro" is commonly used (micrometre per second squared, $\mu\text{m/s}^2$). The gal (or Gal), equal to 1 cm/s^2 , is a derived unit for acceleration in the CGS system of units. A prefix of "milli" is commonly used (milligal, mGal). In rare cases in the literature, a "gravity unit" (gu) may be encountered. In this publication, the $\mu\text{m/s}^2$ has been the preferred unit for gravity measurements, but mGal has been accepted.

$$\begin{aligned}1 \mu\text{m/s}^2 &= 10^{-6} \text{ m/s}^2 \\1 \text{ mGal} &= 10 \mu\text{m/s}^2 \\1 \text{ gu} &= 1 \mu\text{m/s}^2\end{aligned}$$

The gravity gradient is a gradient of acceleration and so the appropriate units are acceleration units divided by distance units. Thus, "per second squared" (s^{-2}) is appropriate in the SI system. Typical gravity gradients measured in exploration are extremely small, and the prefix "nano" is appropriate in most circumstances (per

nanosecond squared, ns⁻²). The eotvos unit (Eo), although not recognised in either the SI or CGS systems, is used almost universally in geophysics as the unit for gravity gradient measurements. It is equal to 1 ns⁻². In this publication, the ns⁻² and Eo have both been accepted as units for gravity gradient measurements.

$$1 \text{ ns}^{-2} = 10^{-9} \text{ s}^{-2}$$

$$1 \text{ Eo} = 1 \text{ ns}^{-2}$$

Acknowledgments

The Airborne Gravity 2004 Workshop Organising Committee would like to acknowledge the support of the ASEG-PESA 2004 Conference Organizing Committee and the Conference Secretariat. Support from Geoscience Australia, BHP Billiton and the NSW Department of Primary Industries - Mineral Resources helped to make the workshop a success. The diligence of Mario Bacchin, Katharine Hagan, Angie Jaensch, Jim Mason, Peter Milligan, Ian Hone and Roger Clifton enabled this Record to be produced in time for the Workshop, despite a tight deadline. Finally, a vote of thanks goes to the speakers who committed their time and energy to deliver presentations on the day and to compose this permanent record of the event.

Airborne gravity data acquisition and processing: A case study in the Prince Charles Mountains, East Antarctica

Mark McLean
University of Melbourne, Australia
m.mclean@pgrad.unimelb.edu.au

Detlef Damaske, Volkmar Damm and Gernot Reitmayr
Bundesanstalt für Geowissenschaften und Rohstoffe, Hannover

Introduction

The Lambert Glacier/Amery Ice Shelf in East Antarctica is a north-northeast trending graben which extends inland for at least 700 km (Figure 1) (Wellman and Tingey, 1976; Kurinin and Grikurov, 1982; Stagg, 1985). This graben is inferred to represent a failed rift emanating from a triple point or four armed junction between India and Antarctica (Stagg, 1985) either before (Lisker et al., in press) or during the break-up of Gondwana (Boger and Wilson, 2003). While the present configuration of this structure suggests a failed rift, recently proposed models suggest that the Lambert region also preserves evidence of an earlier Cambrian suture between at least two Pre-Cambrian blocks that collided during the assembly of Gondwana (Boger et al., 2001). Although sporadic outcrops in the north yield some geological information, large areas to the south are covered with ice rendering it inaccessible to geological sampling (Figure 1).

This paper describes the acquisition and preliminary processing phases of an airborne gravity, magnetic and ice-penetrating radar survey undertaken during the Prince Charles Mountains Expedition of Germany and Australia 2002/03 (PCMEGA). PCMEGA was Australia's first airborne geophysical investigation in the Antarctic continent. This expedition consisted of a field leader, five members of a traverse team, five geophysicists, thirteen geologists, three surveyors, one glaciologist, three field training officers, one doctor, and six members in a helicopter and twin otter crew. From a geophysical perspective, the objective of this investigation was to further our understanding of the Lambert / Amery Rift system and its possible extension underneath the polar ice cap.

Acquisition and Processing

The study area covered part of the southern Prince Charles Mountains, from approximately 72° 45' S to 77° 30' S and 62° E to 72° E (Figure 1). A total of 29 844 km of survey data at 5 km line spacing and 25 km tie-line spacing was acquired over an area of approximately 81 000 km². The tie-line spacing of 25 km (i.e., 1:5 ratio of flight line to tie-line spacing) was chosen to combat the unusually high magnetic diurnal effects at high latitudes. The main grid extended over 350 km, from Wilson's Bluff to 78° S. More lines were flown over an area 150 km by 60 km to the west of the main grid (Figure 1).

The gravity, magnetic and ice-penetrating radar equipment were installed in a De Havilland DHC-6-300 Twin Otter aircraft (Figure 2).

The ice radar was capable of detecting the bedrock to a maximum depth of 3600 metres below the ice surface. To enable the thickest parts of the ice sheet to be accurately surveyed, it is desirable to acquire ice radar data using a drape surface with minimum constant terrain clearance. The ice radar yields an acceptable performance within a terrain clearance range of 200 m and 800 m above ground level.

In contrast to the requirements imposed by the ice radar equipment, the gravity system used for this survey needed to be flown at a constant elevation. Since the ice sheet increases in thickness towards the south, there are conflicting requirements in terms of an optimum drape surface when collecting gravity and ice radar data simultaneously. This conflict was resolved by dividing the survey into three blocks. Each block was flown with a constant flight elevation: 2160 m in the northern block, 2760 m in the central block and 3360 m in the southern block (Figure 3) (all heights referenced to the WGS84 ellipsoid). As the aircraft approached terrain clearance limits of 200 m or 800 m above the ice surface, depending on whether a line was being flown north to south or south to north, the aircraft elevation was increased or decreased by 600 m to the elevation required for the next block. The gravity meter was clamped during each change in elevation. It took several minutes for the gravity meter to settle after this change, so there was a data gap of 10 to 15 km for each a step in elevation. The gaps in the gravity images are a reflection of these data gaps.

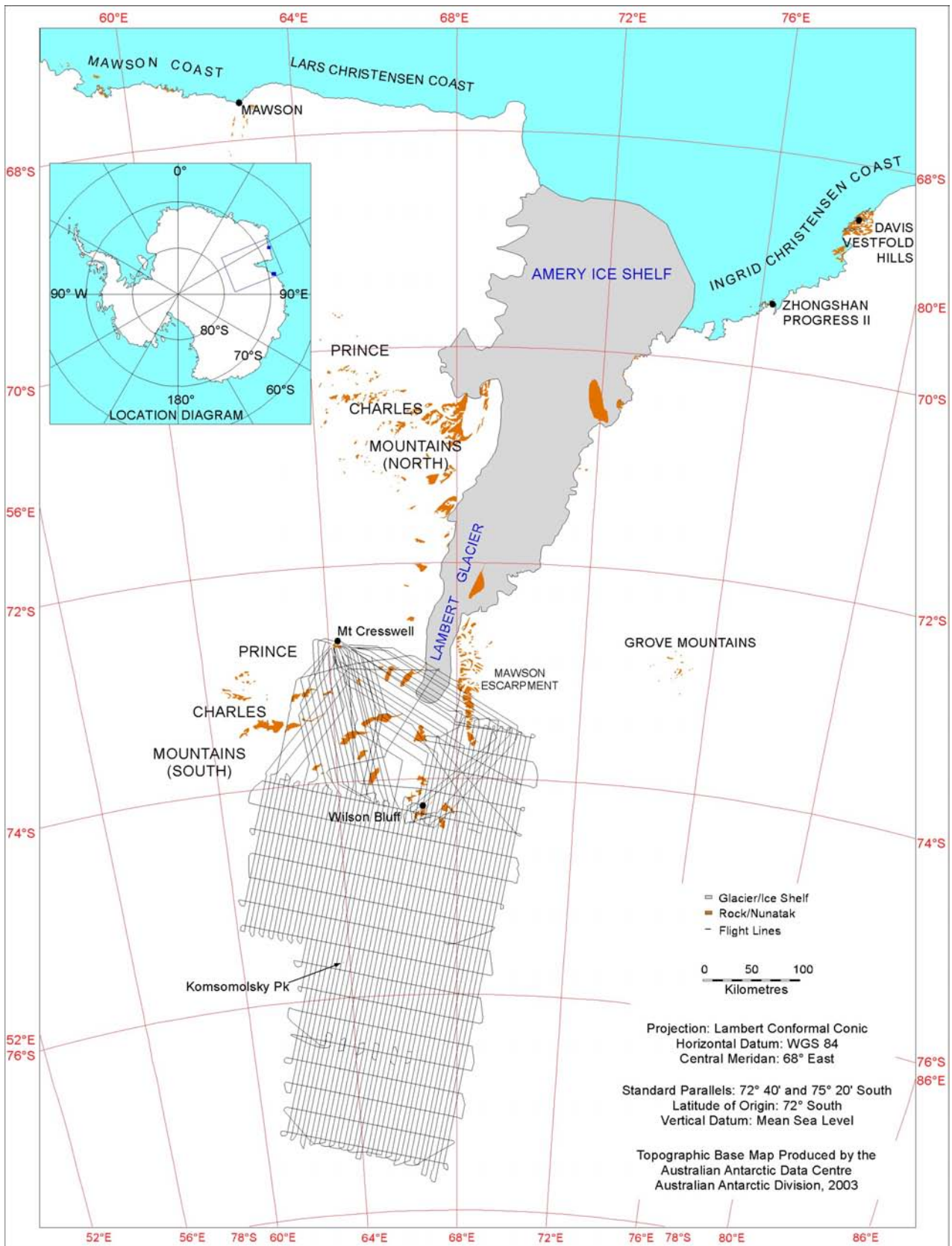


Figure 1. Location map for the PCMEGA survey in the Prince Charles Mountains. The locations of flight lines are shown as black lines.

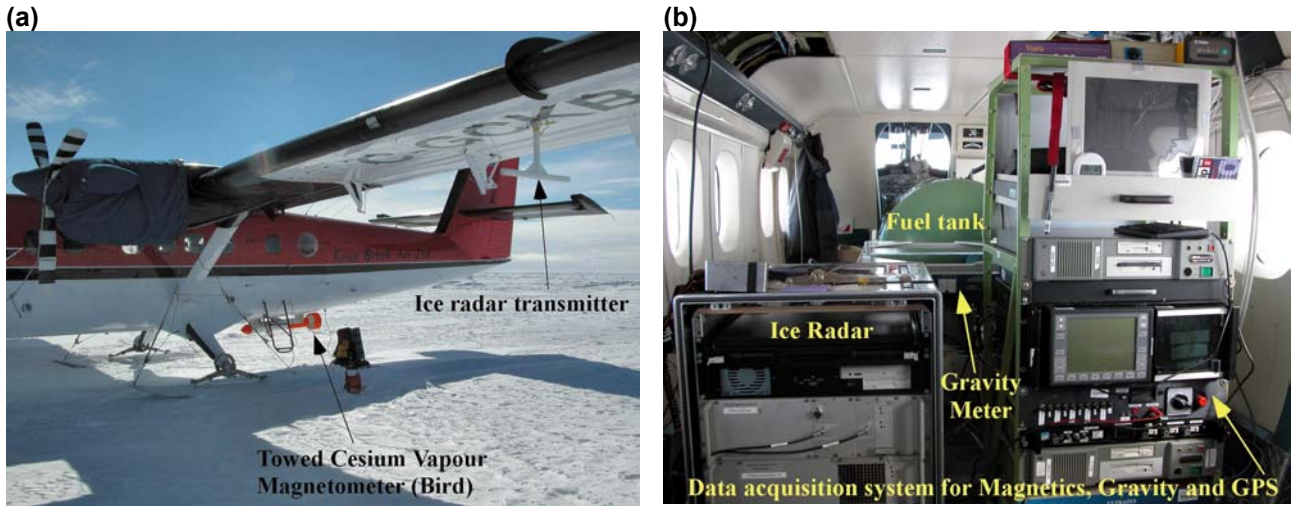


Figure 2. (a) External view of the De Havilland DHC-6-300 Twin Otter data acquisition aircraft at Mt Cresswell base. The bird is housed underneath the aircraft and the ice radar transmitter is fixed to the underside of the wing. (b) Arrangement of equipment inside the aircraft.

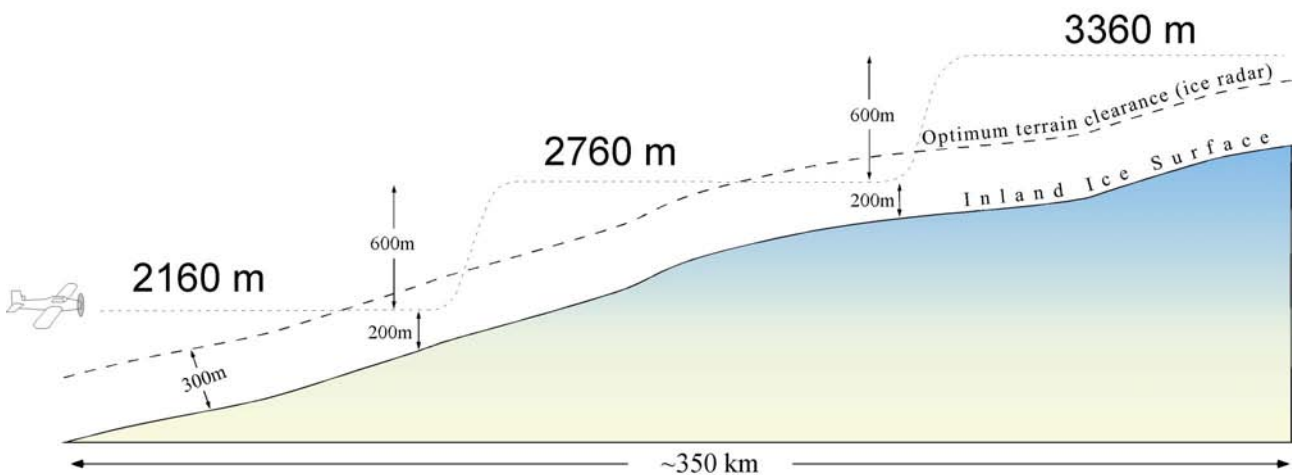


Figure 3. Schematic diagram of drupe surface whereby data were collected at three elevation levels: 2160 m, 2760 m, and 3360 m above the WGS84 ellipsoid. The gravity system used for this survey required acquisition at constant elevation whilst the ice radar required a terrain clearance of 200 to 800 m.

A cesium vapour magnetometer in a towed bird (Figure 2a) was used to acquire magnetic data. These data were subject to de-spiking, followed by the application of diurnal, IGRF, levelling and micro-levelling corrections. A low-pass filter of length 50 s was then applied. An image of total magnetic intensity is shown in Figure 4. The filtering was far more severe than would normally be applied due to the elevated level of diurnal activity that occurs at high latitudes. The impact of the filtering was, however, diminished by the anticipated minimum depth to magnetic source (i.e., the minimum depth to bedrock) of at least 1000 m.

The airborne gravity system consisted of a ZLS Ultra-Sys Air/Marine upgrade LaCoste and Romberg ‘S’ Meter mounted on a vibration isolation platform (Williams and MacQueen, 2001). The gravity sensor was located on the aircraft centreline, just aft of the auxiliary fuel tank (Figure 2b). This position was chosen because it is close to the aircraft’s centre of gravity. The gravity meter has a working range of 0 - 20,000 mGal, a sensitivity of 0.1 mGal and an operating temperature range of -20 to +45 °C. Gravity measurements were made at a frequency of 1 Hz (approximately 70 m).

Two LaCoste and Romberg G-type meters were used to take base station and calibration readings prior to commencement and at the end of the survey at the Mt Cresswell base. These calibration procedures were used to determine the gravity meter drift over the survey time period and to ensure that the system was functioning properly.

Initial processing of the gravity data to the stage of free-air anomaly values was carried out by the equipment supplier (Baron-Hay et al., 2003). In calculating the free-air gravity anomaly values, a number of corrections were applied to the measured gravity values. These included a drift correction, the theoretical gravity correction based on the IGSN71 gravity datum and 1967 International Gravity Formula, the airborne Eötvös correction, and the free-air anomaly correction. A tidal correction was considered unnecessary since the survey area was so close to the pole. Several other corrections such as for vertical accelerations calculated from GPS measurements were applied, but the details of these corrections were considered proprietary by the contractor. Details of the low-pass filter applied to the data are yet to be received. After these processes were carried out, the data were levelled and gridded with a 1000 m cell size.

Bouguer corrections

Taking the contractor-supplied free-air anomaly values and deriving a meaningful Bouguer anomaly map in an ice covered terrain is complicated by the need to take the ice thickness and density into account as well as the surface topography and the density of the bedrock. The simple Bouguer correction needs to be calculated in two stages; first applying a standard Bouguer slab correction based on the surface elevation and a density value chosen for bedrock, then an adjustment to this correction to account for the thickness and density of the ice layer (Torge, 1989; Reitmayr, 2003).

Simple Bouguer anomaly values are derived by calculated the effect of an infinite horizontal slab extending between the elevation datum and the ground surface vertically below each measurement point:

$$g_{SBA\Box} = 0.04192 \rho_b \cdot h \quad (\text{Equation 1})$$

where g_{SBA} is the simple Bouguer correction (mGal), ρ_b is the mean density of the slab (in g/cm^3 , with a value of 2.67 g/cm^3 typically used) and h is the surface elevation in metres above the geoid (Torge, 1989; Reitmayr, 2003). Once the simple Bouguer correction has been calculated for each geographic locality, it is subtracted from the free-air gravity value.

A correction can then be applied to account for the density of ice relative to the density assigned to the slab:

$$g_{ice\Box} = -0.04192(\rho_b - \rho_{ice}) \cdot t_{ice} \quad (\text{Equation 2})$$

where g_{ice} is the correction for the presence of ice (mGal), ρ_b is the density used in the simple Bouguer correction (2.67 g/cm^3 in this instance), ρ_{ice} is the density of ice (0.87 g/cm^3 was used in this case) and t_{ice} is the thickness of ice in metres. Subtracting this ice correction from the simple Bouguer anomaly yields simple Bouguer anomaly values corrected for the presence of ice.

As part of the next phase of this investigation, a 2D surface and sub-ice terrain correction will be calculated using Fourier domain terrain modelling techniques described by Parker (1973) and applied by Studinger et al. (2004).

Preliminary observations from the survey

As expected, there is a strong correlation between the free-air gravity (Figure 5) and the sub-ice elevation data derived from the ice radar (Figure 6). A north-east-trending sub-ice valley that enters from the south-west corner of the grid has been interpreted as the extension of the Lambert Rift. In the northern region of the grid, another sub-ice valley underlies the upper Lambert Glacier and extends towards the south-east. We suggest that this valley is the third arm of a triple point proposed by Stagg (1985).

Given the smoothness of the surface topography (Figure 7), it is not surprising that the simple Bouguer anomaly map without ice correction (Figure 8) is similar to the free-air anomaly map (Figure 5). The simple Bouguer anomaly image with ice correction (Figure 9) is quite different to either of these previous gravity images. There is a strong south to north gradient which is likely to reflect deep crust or mantle density variations. The high observed in the free-air gravity associated with the Gamburtsev Mountains is a low in the ice-corrected simple Bouguer anomaly map. Although less obvious, there is a positive Bouguer anomaly that coincides with the rift observed in the ice radar dataset. The appearance of relatively short wavelength features such as this is enhanced by removing a first order trend surface from the ice-corrected simple Bouguer data (Figure 10).

It should be noted that the Bouguer anomaly map is limited by the accuracy of the sub-ice and surface elevation data (Figures 6 and 7, respectively). Since there are discrepancies in both of these datasets, some caution should be exercised when interpreting the Bouguer anomaly data. In a similar airborne geophysical

survey, Studinger et al. (2004) estimated the standard deviation of the errors in the surface elevation values to be 2.7 m and the standard deviation of the errors in the sub-ice elevation values to be 81 m.

Acknowledgments

The PCMEGA project was jointly funded by the Australian Antarctic Division and the Bundesanstalt für Geowissenschaften und Rohstoffe (BGR). The gravity and magnetic equipment was supplied and operated by Fugro Airborne Surveys. Ice penetrating radar equipment was supplied and operated by Dr. Volkmar Damm from the BGR. The Twin Otter aircraft used for the geophysical surveys was owned and operated by Kenn Borek Air, on contract to the Australian Antarctic Division.

References

- Baron-Hay, S., Parsons, M. and Stenning, L. 2003, Antarctic Magnetic and Gravity Geophysical Survey: Acquisition and Processing Report for PCMEGA, Prince Charles Mountains Expedition Germany and Australia: Fugro Airborne Surveys (Unpublished).
- Boger, S.D. and Wilson, C.J.L., 2003, Brittle faulting in the Prince Charles Mountains, East Antarctica: Cretaceous transtensional tectonics related to the break-up of Gondwana: *Tectonophysics*, 367, 173-186.
- Boger, S.D., Wilson, C.J.L. and Fanning, C.M., 2001, Early Paleozoic tectonism within the East Antarctic craton: The final suture between east and west Gondwana?: *Geology*, 29, 463-466.
- Kurinin, R.G., and Grikurov, G.E., 1982, Crustal structure of part of East Antarctica from geophysical data: in Craddock, C. (Ed.), *Antarctic Geoscience*, University of Wisconsin Press, Madison, 895-901.
- Lisker, L., Brown, R. and Fabel, D., In Press, Denudational and thermal history along a transect across the Lambert Graben, Northern Prince Charles Mountains, Antarctica: *Tectonics*.
- Parker, R.L., 1973, Rapid calculation of potential anomalies: *Geophysics J. R. Astron. Soc.*, 31 447-455.
- Reitmayr, G. 2003, Continuation of Gravity Measurements in Victoria Land and at the Oates Coast, Antarctica, during GANOVEX VII: *Ber. Arch. BGR – Hannover*.
- Stagg, H. M. J., 1985, The structure and origin of Prydz Bay and MacRobertson Shelf, East Antarctica: *Tectonophysics*, 114, 315-340.
- Studinger, M., Bell, B.E., Buck, R.W., Karner, G.D. and Blankenship, D.D., 2004, Sub-ice geology inland of the Transantarctic Mountains in light of new aerogeophysical data: *Earth and Planetary Science Letters*, 220, 391-408.
- Torge, W., 1989, *Gravity*: Berlin, New York (W. de Gruyter).
- Wellman, P. and Tingey, R.J., 1976, Gravity evidence for a major crustal fracture in east Antarctica: *BMR Journal of Australian Geology and Geophysics*, 1, 105-108.
- Williams, S., and MacQueen, J.D., 2001, Development of a versatile, commercially proven, and cost-effective airborne gravity system: *The Leading Edge*, 20, 651-654.

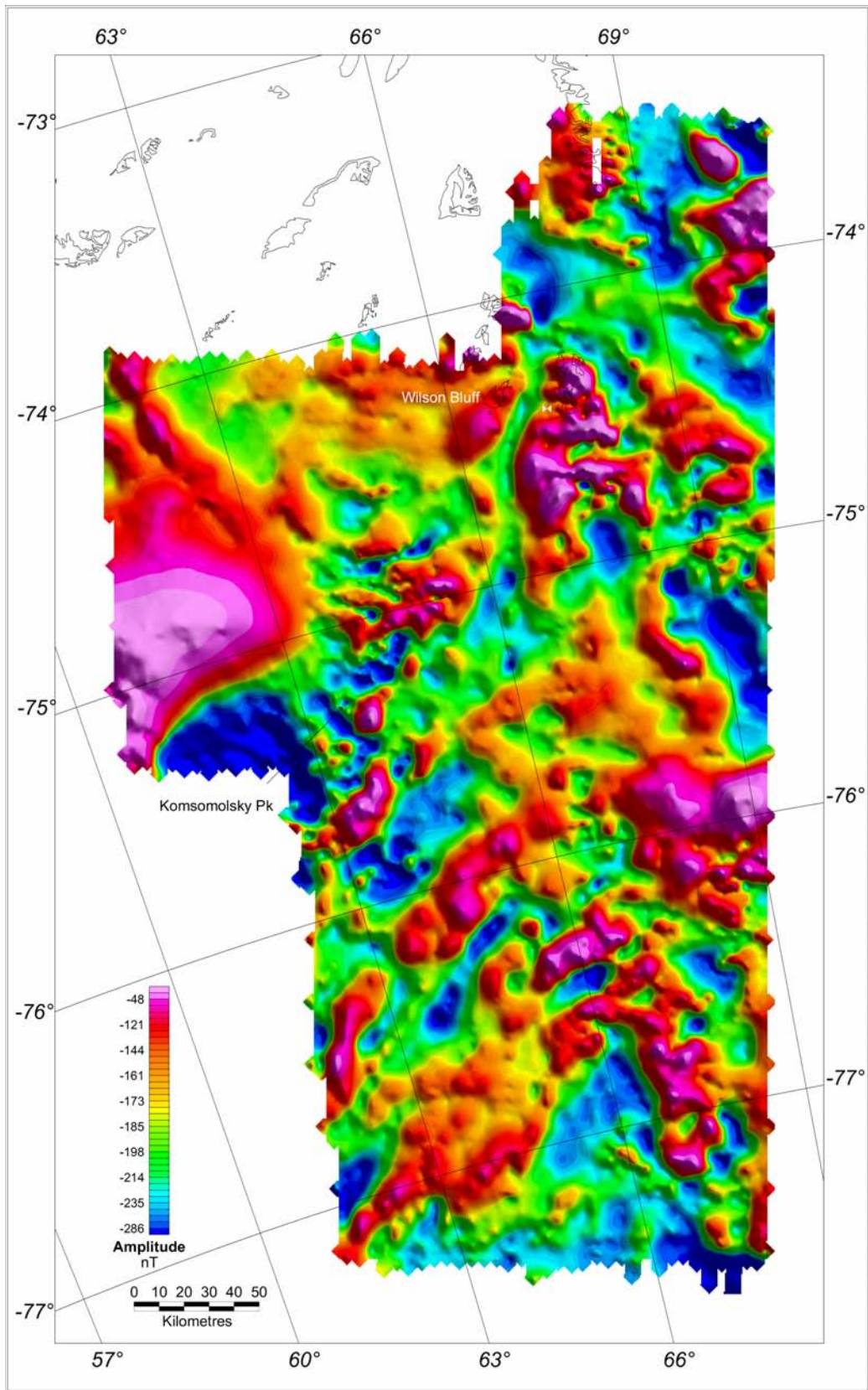


Figure 4. Total magnetic intensity image for the Southern Prince Charles Mountains.

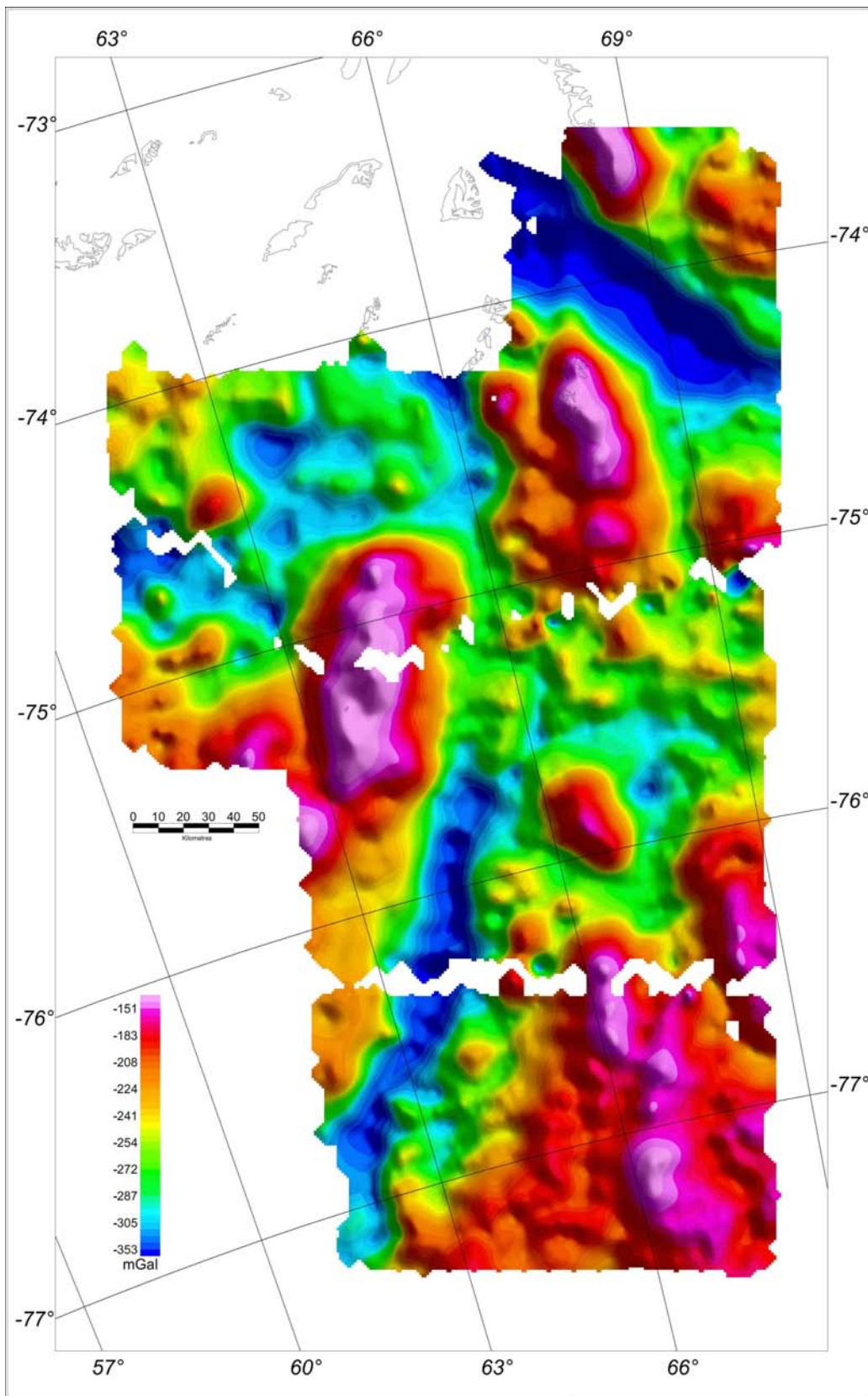


Figure 5. Free-air gravity map for the Southern Prince Charles Mountains.

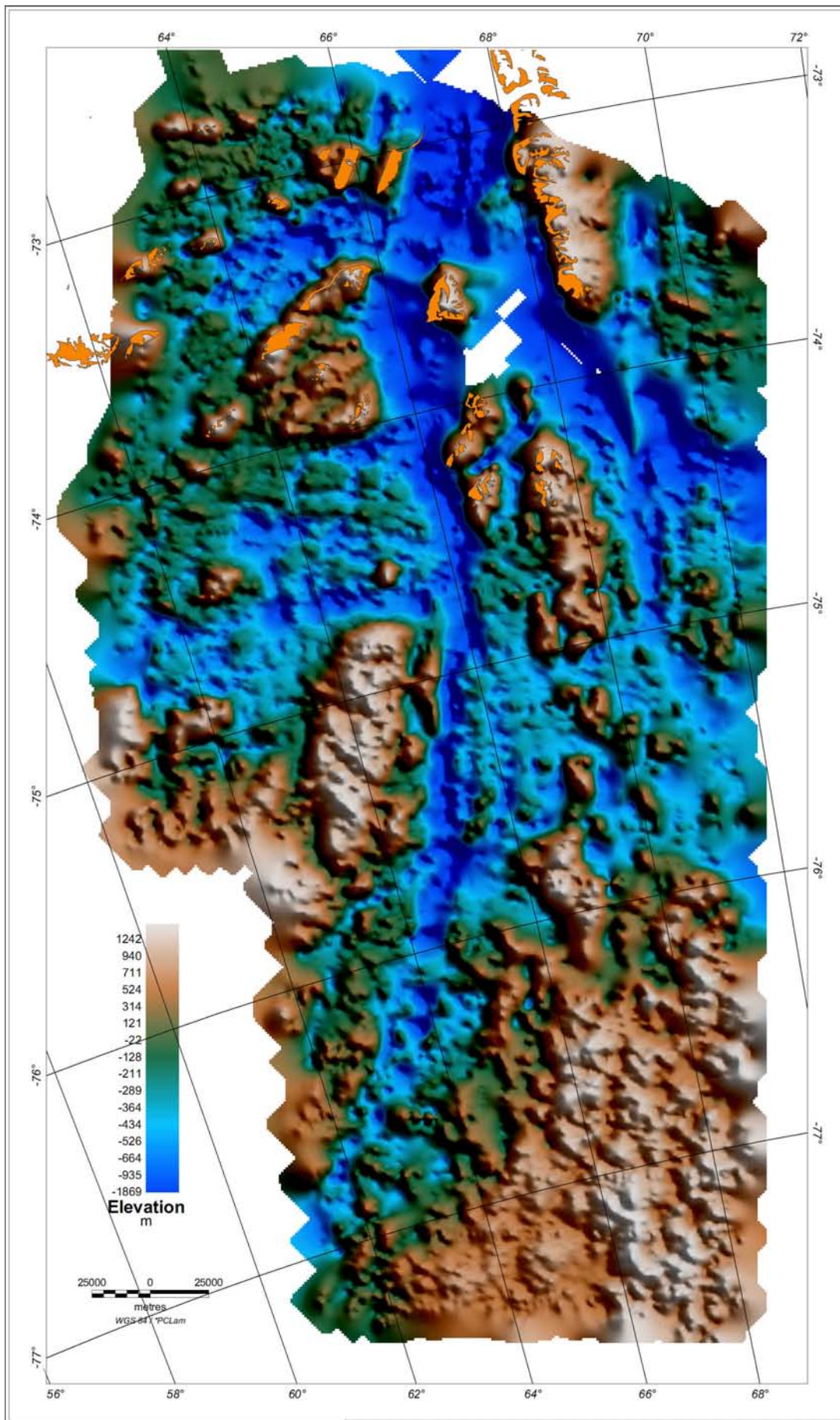


Figure 6. Sub-ice elevation map for the Southern Prince Charles Mountains. Maximum ice thickness is approximately 3776 m and mean ice thickness is approximately 1720 m.

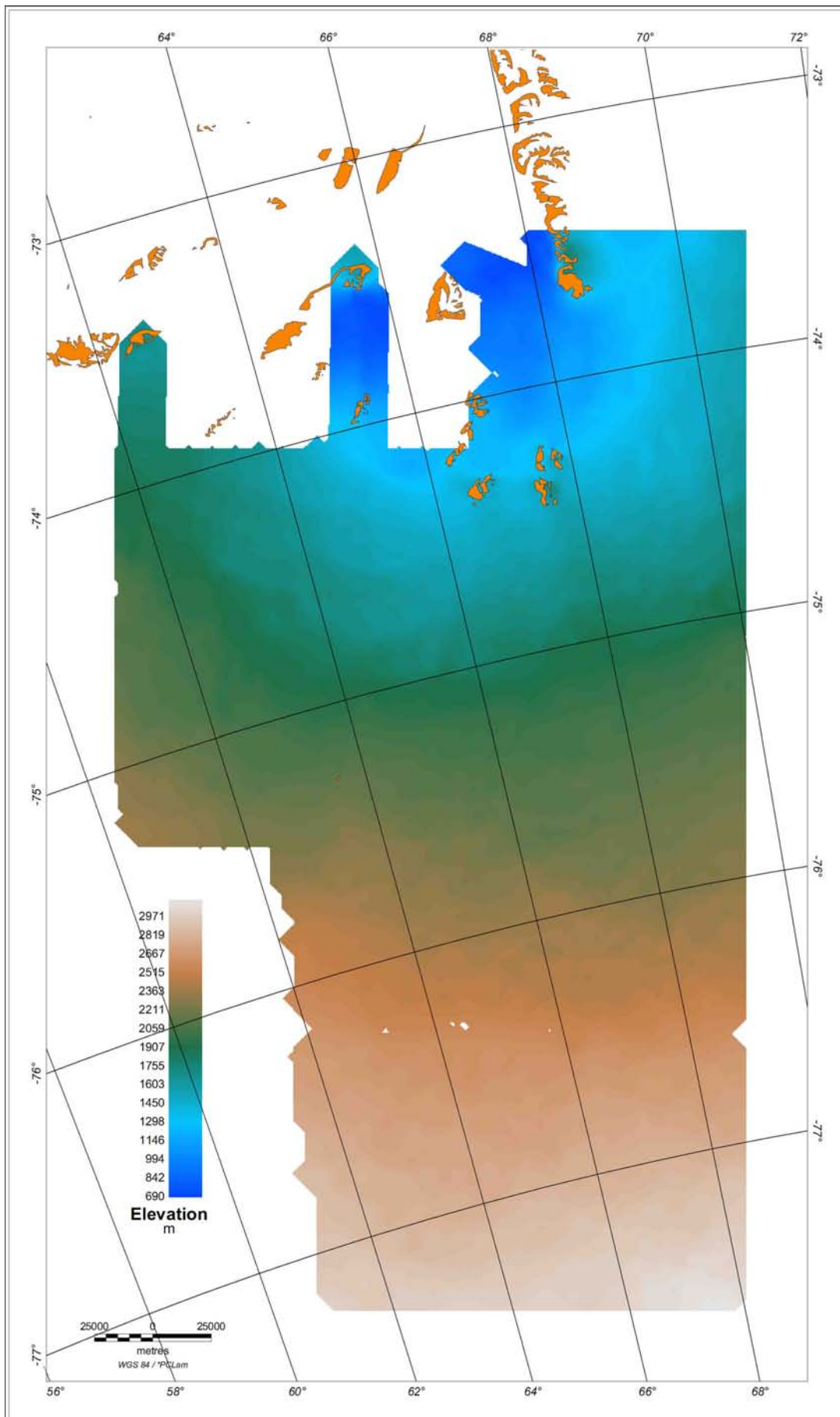


Figure 7. Surface elevation map for the Southern Prince Charles Mountains.

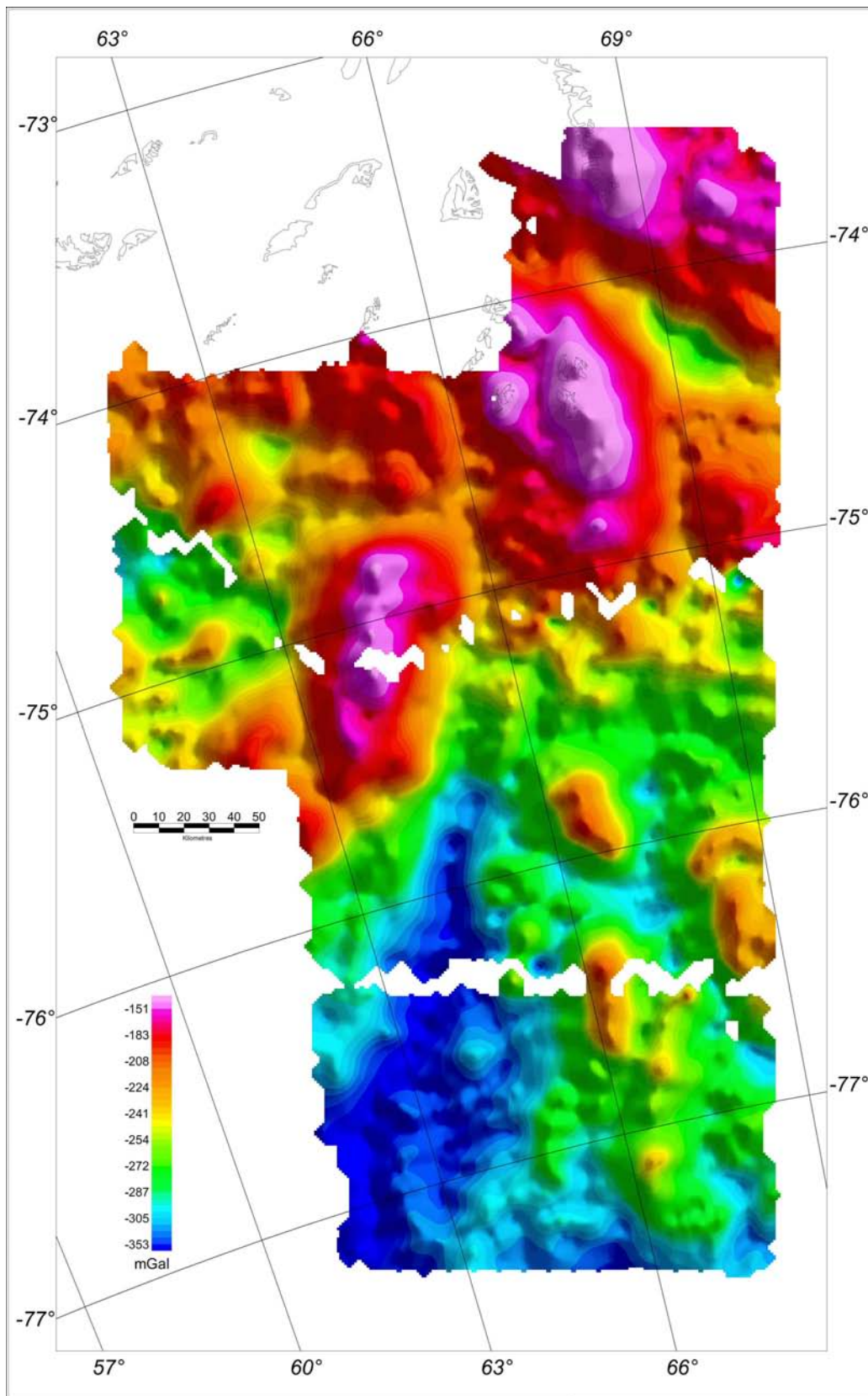


Figure 8. Simple Bouguer anomaly map (without ice correction) for the Southern Prince Charles Mountains

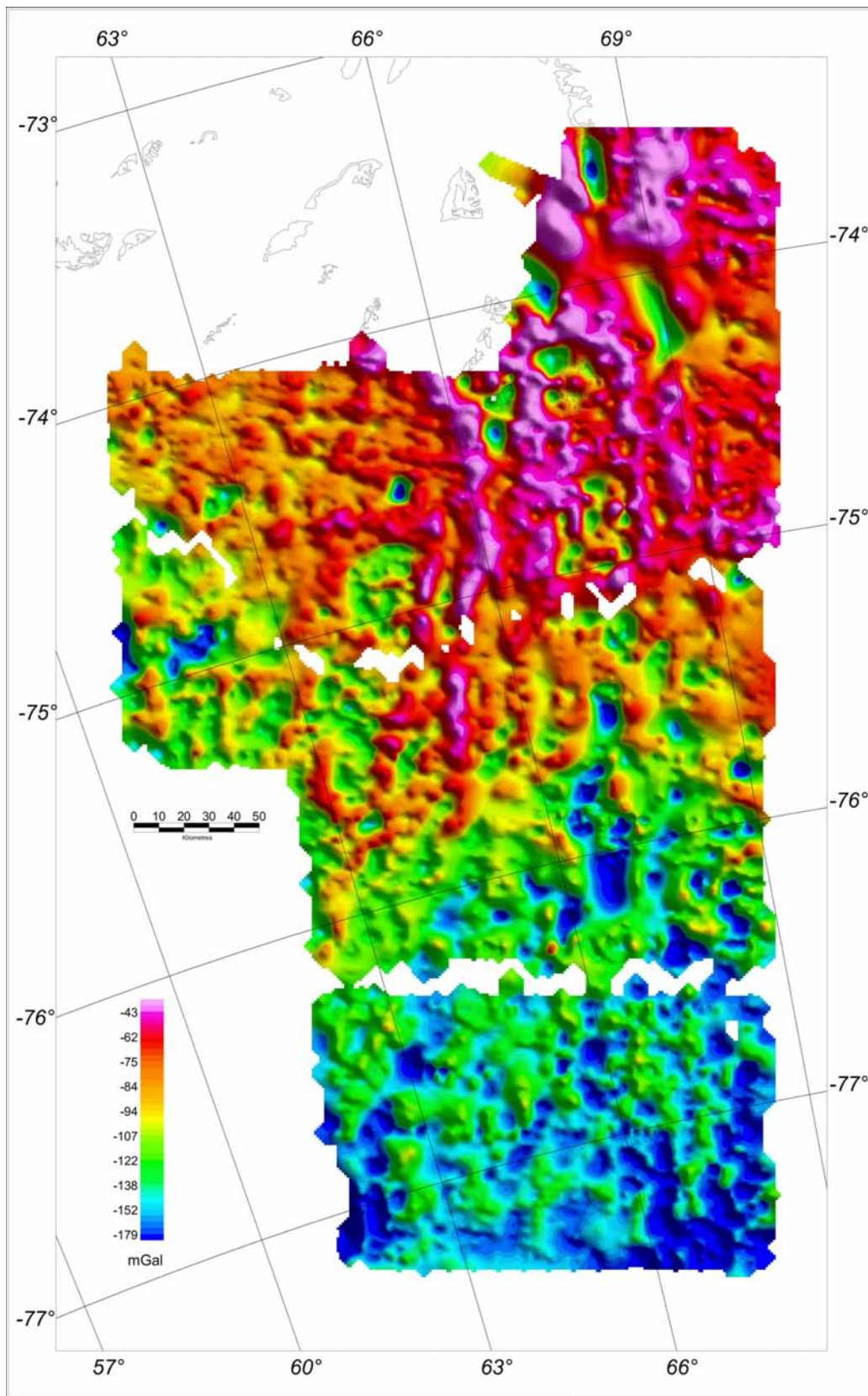


Figure 9. Simple Bouguer anomaly map (with ice correction) for the Southern Prince Charles Mountains.

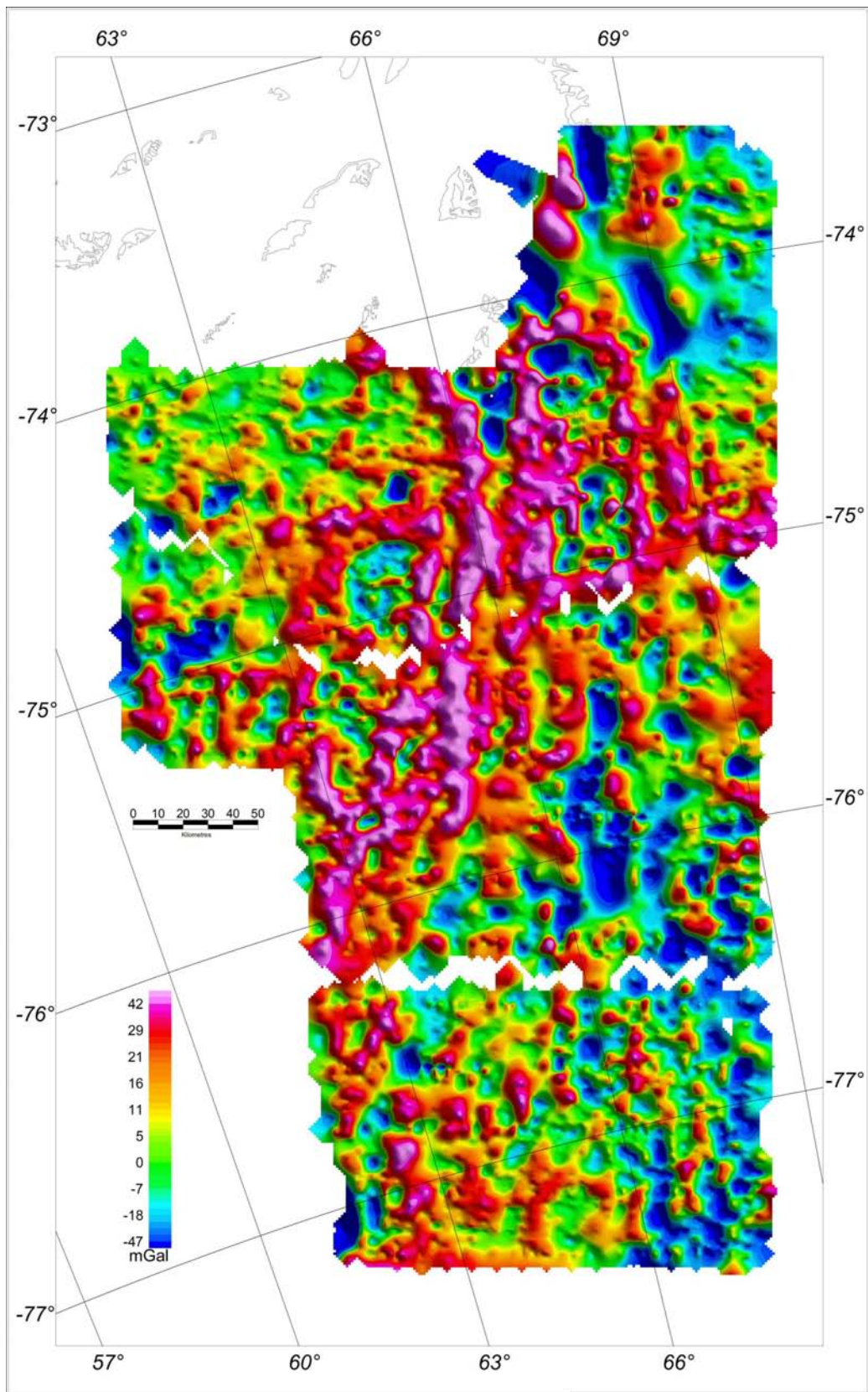


Figure 10. Residual simple Bouguer anomaly map (with ice correction) for the Southern Prince Charles Mountains after removing a first order trend surface.